

End-Point Positioning of One-Link Flexible Arm under Translational Motion

SeongCheol Lee*, Seiji Chonan** and Hikaru Inooka**

* Department of Mechanical Engineering
Chonbuk National University, Chonju, Korea

** Department of Mechanical Engineering
Faculty of Engineering
Tohoku University, Sendai, 980 Japan

ABSTRACT

A theoretical and experimental study of a single link flexible arm with a tip mass is presented for the translational end-point positioning. The problem of shifting the end-point from its initial position to the commanded position by the amount of w_0 is considered for the open loop control such that the base follows up the given path function. The theoretical results are obtained by applying the method of the Laplace transform to the governing equation, and the solution is calculated by the method of numerical inversion. Experimental results are obtained and compared with the theoretical ones.

1. INTRODUCTION

In the past few years, the requirements of high performance on industrial robots have led to the consideration of structural flexibility in robot arm. In this case, one has to make the moving parts of arm more lighter. However due to the flexibility of arm, the oscillation are generated and the assumptions for the rigid arm are no longer applicable. One then has to control the arm so that the vibration is not induced and the high speed positioning is achieved.

Many papers have been published on the flexible arms during the past few years. Cannon and Schmitz, (1) Skaar and Tucker, (2) Yuh, (3) Tahara and Chonan, (4) et al. studied the open-loop and the closed-loop end-point controls of a single link flexible manipulators. But most of these papers concerned with the rotational motion and only a few papers of S. Hur (5), Lee, Chonan and Inooka (6), Sasaki and Inooka (7), K.H. Yu (8) dealt with translational motion of the flexible arm.

In this paper, the end-point positioning of a one link flexible arm with a tip mass under the translational movement is studied analytically and experimentally. The beam is mounted on a translational mechanism driven by the ballscrew, whose rotation is controlled by the DC servomotor. The problem of shifting the end-point from the initial position to the commanded position is studied for the open loop control to use the given path functions as input to the base movement. In this case, the displacement of the end-point is measured according to the variations of the rising time of base movement up to the desired position.

The governing equation of system is constructed

based on the Bernoulli-Euler theory. The solution for the governing equation is obtained by applying both the method of the Laplace transform and the Numerical inversion method proposed by Weeks (9). The numerical and experimental results are presented here.

2. FORMULATION AND ANALYSIS

Figure 1 shows the single link flexible arm studied in this analysis. It is composed of a DC servomotor, a ballscrew mechanism, a flexible arm of length L and an end-point payload. The base of the arm is translated by the ball screw driven by the motor. As shown in the figure, the x -axis is placed along the axis of the arm and the z -axis is normal to the x -axis. And the y -axis is perpendicular to both the x - and z -axes. One assumes that the arm deflection is seen only in the x - z plane.

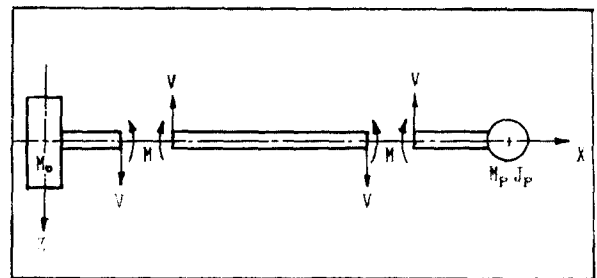


Figure 1. Geometry of Flexible Arm and Coordinates

In this model, denoting the lateral displacement of the arm by $w(x,t)$, the governing equation of the arm by Bernoulli-Euler beam theory is written as

$$(1) \quad EI(1+C\frac{\partial}{\partial t})\frac{\partial^4 w(x,t)}{\partial x^4} + \rho A \frac{\partial^2 w(x,t)}{\partial t^2} = 0$$

where E is the Young's modulus, ρ is the mass density, I is the moment of inertia, A is the cross-sectional area, C is the internal damping coefficient of the arm, and t is time.

One next considers the boundary conditions of the arm displacement and force equilibrium at $x=0$ and $x=L$ respectively and brings in the geometrical relations of ballscrew. Then one can get the following equations (2) to (6).

$$(2) \quad w(0,t) = 0 \quad \frac{\partial w(0,t)}{\partial t} = 0$$

$$(3) \quad M_0 \frac{\partial^2}{\partial t^2} w(0, t) + C_s \frac{\partial}{\partial t} w(0, t) = R + V$$

$$(4) \quad J_p \frac{\partial^2}{\partial t^2} \left(\frac{\partial w(L, t)}{\partial x} \right) = -EI \left(1 + C \frac{\partial}{\partial t} \right) \frac{\partial^2 w(L, t)}{\partial x^2}$$

$$(5) \quad M_p \frac{\partial^2 w(L, t)}{\partial t^2} = EI \left(1 + C \frac{\partial}{\partial t} \right) \frac{\partial^3 w(L, t)}{\partial x^3}$$

$$(6) \quad P_t \cos \phi = R \sin \phi + \mu (P_t \sin \phi + R \cos \phi)$$

where M_0 is the mass of the pedestal, C_s is damping coefficient between base and ballscrew, R is the reaction force between the pedestal and the screw, V is the shear force from the arm. P_t , μ and ϕ are the radial force acting on the ballscrew from the pedestal, the friction coefficient and the lead angle of ballscrew respectively. M_p is the mass of the payload and J_p is the polar moment of inertia of the payload around the y-axis. Next, the equilibrium of moment around the motor shaft is given

$$(7) \quad J_m \frac{\partial^2 \theta}{\partial t^2} = -\frac{\partial \theta}{\partial t} - Pr + T$$

where J_m is the inertia moment of the motor shaft, ε is the damping coefficient of motor shaft, θ and r are the rotational angle and the radius of ballscrew respectively. And the torque T applied by the motor is given by

$$(8) \quad T = K_t i_a$$

where i_a is the armature current and K_t is the torque constant of the motor. To get the arm motion under control, one has to prescribe the armature current i_a in the motor circuit. For this purpose, one gives the path function to the base by means of computer as an input which makes the end-point move to the commanded tip position w_d , which is measured by a sensor. This input of path function is used as the basis for applying torque to the arm base through the motor. The circuit equation to the current i_a to be controlled is

$$(9) \quad \frac{L_a}{R_a} \frac{di_a}{dt} + i_a + \frac{E_b}{R_a} = G_d w_d(0, t)$$

where L_a is the motor inductance, R_a is the circuit resistance of motor armature, E_b is the back electromotive force, G_d is displacement gain, $w_d(0, t)$ is the desired position.

One solves the problem by applying the method of the Laplace transform with respect to time. Assuming that the arm is resting statically at $t=0$, one has the Laplace transformed equation of (1), which is simplified as

$$(10) \quad \frac{\partial^4 W(x, s)}{\partial x^4} - \zeta^4 W(x, s) = 0$$

$$\text{where } \zeta^4 = -\frac{\rho A s^2}{EI(1 + C_s)}$$

Then, the general solution of equation (10) is given by

$$(11) \quad W(x, s) = a \sin \zeta x + b \cos \zeta x + \gamma \sinh \zeta x + \delta \cosh \zeta x$$

Here, s is the Laplace transform parameter, a to δ are unknown constants to be determined from the boundary conditions. Substituting equation (10) into the transformed equations of (2)-(8), and further introducing the transformed current $I_a(s)$ obtained from equation (9) into the resulted equations, one has a type of simultaneous algebraic equations of the form

$$(12) \quad [a_{ij}][\alpha, \beta, \delta]^T = [W_d(0, s) \quad 0 \quad 0]^T$$

where $W_d(0, s)$ is the commanded position of the arm base, which is given by amplitude of the path function and is also the same amount of the displacement as the end-point at the statical state of arm. a_{ij} , ($i, j = 1, 2, 3$) are given in the Appendix. After having α , β , and δ from equations (12), one has the transformed displacement represented by W_d as

$$(13) \quad \frac{W(x, s)}{W_d(0, s)} = \frac{1}{\Delta} \{ \Delta \alpha (\sin \zeta x - \sinh \zeta x) + \Delta \beta \cos \zeta x + \Delta \delta \cosh \zeta x \}$$

where $\Delta \alpha$, $\Delta \beta$, $\Delta \delta$, Δ are follow as

$$\begin{aligned} \Delta \alpha &= a_{22}a_{33} - a_{23}a_{32} \\ \Delta \beta &= a_{23}a_{31} - a_{21}a_{33} \\ \Delta \delta &= a_{21}a_{32} - a_{22}a_{31} \\ \Delta &= a_{11}(a_{22}a_{33} - a_{23}a_{32}) + a_{12}(a_{32}a_{31} - a_{12}a_{33}) \\ &\quad + a_{13}(a_{12}a_{32} - a_{22}a_{31}) \end{aligned}$$

Since one considers the path function $P(t)$ applied to the arm base, the desired function is given by

$$(14) \quad w_d(t) = w(0, t) = W_d * P(t)$$

Finally, the input-output equation for the open loop translational positioning is written by

$$(15) \quad \frac{W(x, s)}{W_d * P} = \frac{1}{\Delta} \{ \Delta \alpha (\sin \zeta x - \sinh \zeta x) + \Delta \beta \cos \zeta x + \Delta \delta \cosh \zeta x \} P(s)$$

In the numerical examples, one calculates the inverse integral of equation (15) by the numerical method proposed by Weeks⁽⁹⁾.

3. EXPERIMENT

Figure 2 is shown the whole experimental setup. The actuator is a DC servomotor (Sanyo Denki U508T) which is driven by the armature current controlled by the computer input. Since the current signal is fed back to the motor armature, the base of arm is moved through the ball screw mechanism translationally. The physical parameters of the motor are

$$\begin{aligned} J_m &= 1.688 \times 10^{-4} \text{ kgm}^2 \\ \varepsilon &= 4.9581 \times 10^{-3} \text{ kgm}^2/\text{s} \end{aligned}$$

$$\begin{aligned}
 K_t &= 1.8829 \times 10^{-1} \text{ Nm/A} \\
 K' &= 3.1194 \times 10^{-1} \text{ V/rad} \\
 L_a &= 5.5 \times 10^{-3} \text{ H} \\
 R_a &= 8.7 \text{ } \Omega
 \end{aligned}$$

And the physical parameters of the ballscrew and the flexible arm of an aluminium beam with a rectangular cross section of thickness B and width H to be used in this experiment are

$$\begin{aligned}
 \rho &= 2.4477 \times 10^3 \text{ kg/m}^2, \\
 r &= 0.0072 \text{ m}, \\
 P_t &= 0.004 \text{ m}, \\
 \mu &= 0.0035, \\
 M_o &= 0.44 \text{ kg}, \\
 B &= 12.10 \times 10^{-3} \text{ m}, \\
 H &= 2.01 \times 10^{-3} \text{ m}
 \end{aligned}$$

$$\begin{aligned}
 \text{arm A: } L &= 0.345 \text{ m} \\
 E &= 6.1986 \times 10^{10} \text{ Pa} \\
 C &= 0.1149 \times 10^{-3} \text{ s} \\
 M_p &= 16.13 \times 10^{-3} \text{ kg} \\
 J_p &= 6.649 \times 10^{-6} \text{ kgm}^2 \\
 \text{arm B: } L &= 0.550 \text{ m} \\
 E &= 4.9566 \times 10^{10} \text{ Pa} \\
 C &= 0.3910 \times 10^{-3} \text{ s} \\
 M_p &= 30.94 \times 10^{-3} \text{ kg} \\
 J_p &= 1.275 \times 10^{-6} \text{ kgm}^2
 \end{aligned}$$

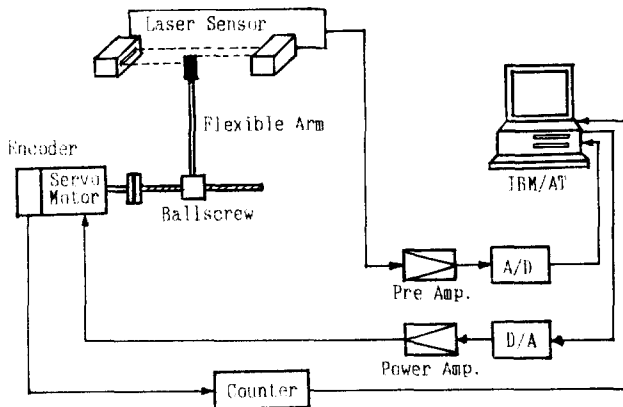


Figure 2. Experimental System

The tip displacement of the arm is measured by a laser beam sensor (Keyence LX-130T), which is set in space so that the strip of the laser beam between the transmitter and the receiver is partially screened by the vibrating arm tip. After obtaining the transmission constant of the voltage to the displacement, one can determine the tip displacement from the output of the sensor. The voltage signal from the sensor is then amplified by the preamplifier (Max. 15V) and put into a 12 bit A/D converter. After that, the digitized signal is sent to a microcomputer (IBM/AT Compatible) to know the end-point position. The output signal from the computer is transferred to a voltage signal through a 12 bit D/A converter. It is then converted to a current through the power amplifier and finally fed back to the armature to drive the motor. The information on the tip displacement is sent to the computer from the laser sensor via the A/D converter every sampling time T_s . Here, in this experiment, T_s was set to 3ms.

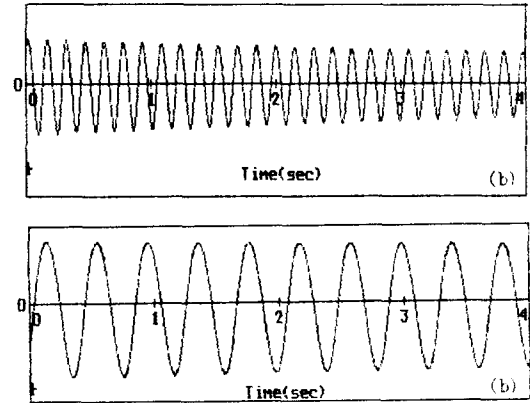


Figure 3. The free vibrations of the flexible arm (experimental results); (a) arm A with natural frequency of 6.5 Hz and 0.01907 logarithmic decrement, (b) arm B with natural frequency of 2.5 Hz and 0.01492 logarithmic decrement.

The free vibrations of the flexible arm A and B as testpieces are shown in figure 3(a) and 3(b). With this figure obtained by experiment, one can get the natural frequency and logarithmic decrement of flexible arm. Figure 3(a) gives the natural frequency of 6.5 Hz and 0.01907 logarithmic decrement of arm A. Figure 3(b) also gives the natural frequency of 2.5 Hz and 0.01492 logarithmic decrement of arm B. One determines the damping factors of arm by using these logarithmic decrements. The longer arm B has bigger flexibility and lower natural frequency than arm A as shown in figure 3.

4. NUMERICAL AND EXPERIMENTAL RESULTS

One introduces a path function which can give the smooth movement to the arm base from the initial position to the desired position without the feedback within the some limited time. The path function used in this paper is given as

$$(16) \quad P(t) = \sin^2 \omega t \quad \begin{aligned} &0 < t \leq \pi/2\omega \\ &= 0 \quad t > \pi/2\omega \end{aligned}$$

To obtain the numerical results, after substituting a Laplace transformed equation of (16) into equation (15), one calculates the end-point displacement $w(L, t)$ to the variation of base movement by applying the numerical method of the inverse Laplace transform proposed by Weeks.

Figure 4 through 9 show the response of the end-point when the path function given by equation (16) is applied to the arm base. Figure 4, as a theoretical results, shows the end-point displacement of arm A and trace of base to the variation of rising time coming to the desired position of base. Figure 5 shows also the end-point displacement obtained by both theoretical and experimental results to the rising time variation. During the period of arriving at the desired position from the initial position, the tip

position obtained by experiment results, as shown in figure 5, follows up the theoretical tip position, which coincides with that of the base very well, with having a little of time phase. In this case, the end-point displacement coincides with the base movement at $t_r=0.52$ very well both theoretically and experimentally. Generally, the rapid reaching of base to the desired position brings on an increment of max. overshoot value. However as shown in figure 4 or 5, one can find that the max. overshoot is first increased within a limited range of time and after then decreased within any range not to be continuing to increase the max. overshoot value according to be shortening of the rising time for the theoretical and experimental results. Figure 4 and 5 show such a state that the increment and decreament of the max. overshoot value are repeating to the variation of rising time. After repeating of this situation, the max. overshoot value continues to increase eventually under the rapid rising time.

Figure 6 shows one example of the theoretical response of tip position for arm B at the fast rising time of base, $t_r=0.1$ second. It has nearly same frequency as the natural frequency of free vibration. The relation between max. overshoot value of the end-point in arm A and the variation of rising time is shown in figure 7. From this relation, one reasonably and approximately finds the optimal rising

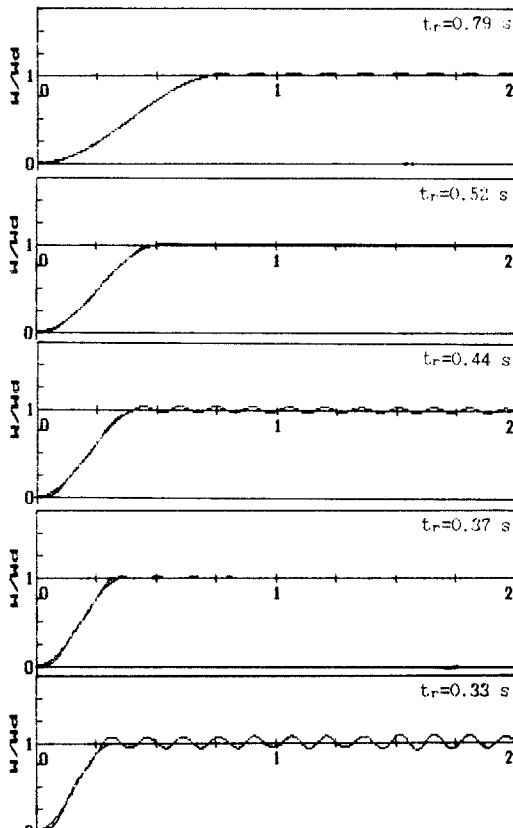


Figure 4. The end-point displacement of arm A and the base movement to the variations of rising time; (theoretical results).

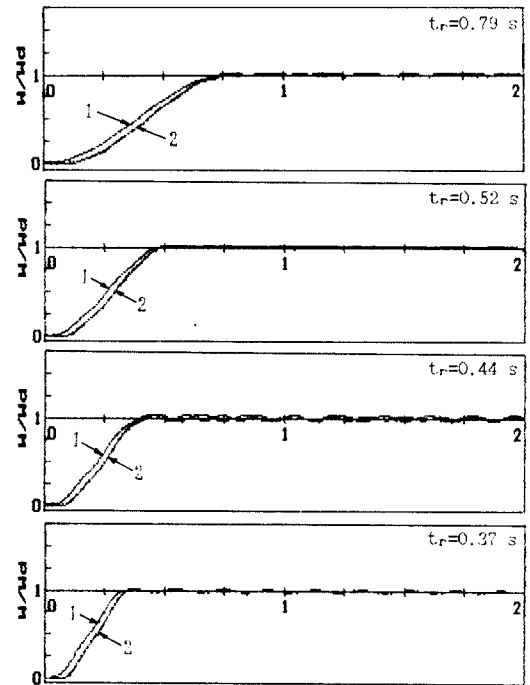


Figure 5. The end-point displacement of arm A obtained by the 1; theoretical and 2; experimental results.

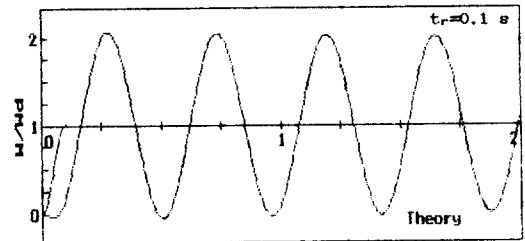


Figure 6. The tip response of arm B to have the fast rising time of base at $t_r = 0.1$ sec. (One theoretical example)

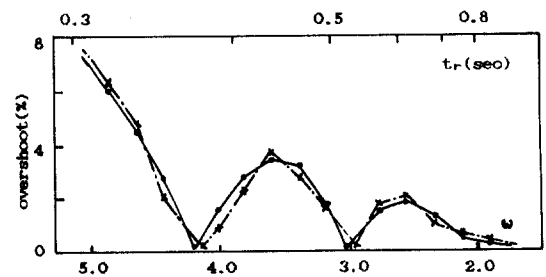


Figure 7. The relation between max. overshoot of the end-point in arm A and variations of base movement. (—•—: Numerical result, ---×---: Experimental result)

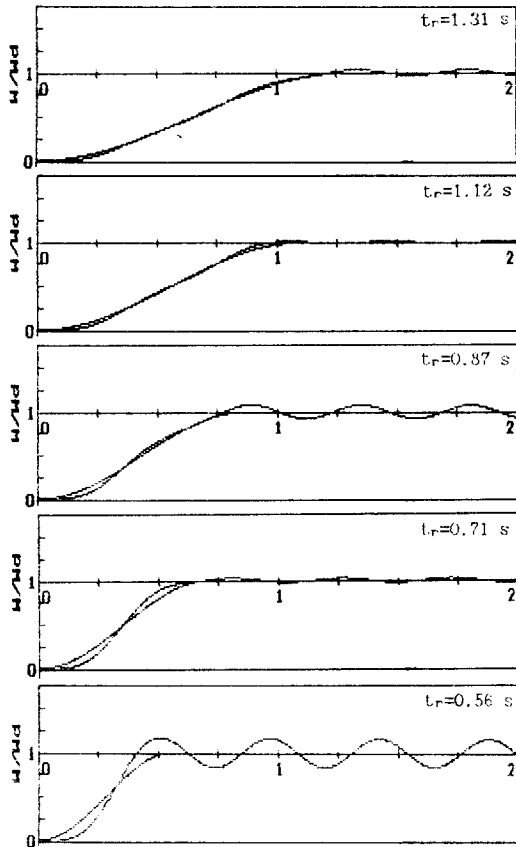


Figure 8. The end-point displacement of arm B and the base movement to the variations of rising time: (theoretical results).

time for base movement not to be generate the vibration without feedback information of the tip displacement by using the numerical results.

Figure 8 and 9 also show the response of the end-point in arm B to the base movement theoretically and experimentally. In this case, it needs a large rising time in order to reach the commanded position without vibration because of the big flexibility of beam and low natural frequency. But it has same inclinations as those of the arm A.

5. CONCLUSIONS

A theoretical and experimental study has been presented for the translational end-point positioning of a one-link flexible arm shifting from its initial position to the commanded position by the amount of w_1 . The flexible arm prototype at the Dept. of Mechanical Engineering of Chonbuk National University has been chosen for developing a simulation study. Results obtained can be summarized as follows.

(1) Translational end-point positioning of one link flexible arm is sufficient to make the arm tip stay at its commanded position within the limited time not to be large by using a path function of base to move

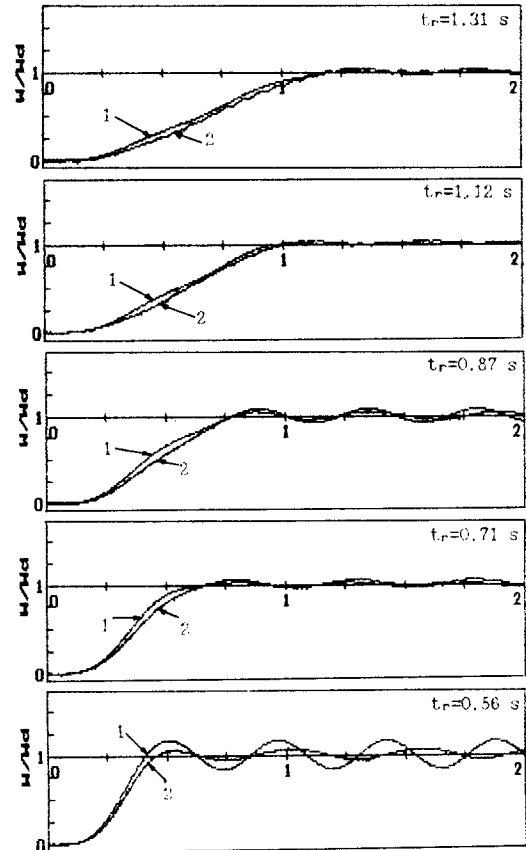


Figure 9. The end-point displacement of arm B obtained by the 1: theoretical and 2: experimental results.

smoothly without feedback information of the end-point even if the arm has a flexibility to be easy to generate the vibration.

(2) Since good agreement between theoretical and experimental results is reasonably obtained, one can find the rapid rising time of base not to be generate the arm vibration by using the numerical results

REFERENCE

- (1) R.H.Cannon and E.Schmitz, "Initial Experiments on the End-point Control of a Flexible one-link Robot," *Int. J. of Robotics Research*, Vol.3, No.3, pp.62-75 (1984)
- (2) S.B.Skarr, D.Tucker, "Point Control of a one-link Flexible Manipulator", *Trans. of the ASME*, Vol.53, pp.23-27 (1986)
- (3) J.Yuh, "Application of Discrete-time Model Reference Adaptive Control to a Flexible single-link Robot," *J. of Robotic Systems*, vol.4, pp.621-630 (1987).
- (4) M.Tahara and S.Chonan, "Closed-loop displacement control of a one-link flexible arm with a tip mass" *JSME Int. J.*, Vol.31, No.2, pp.409-415 (1988)
- (5) S.Hur, "Translational Control of a 1-link Elastic Arm with a Tip Mass," MS.D. Thesis, Feb.1989, Chonbuk National University. (In Korean)

- (6) S.C. Lee, S.Chonan, and H.Inooka, " Translational control of a one-link flexible arm" '89KACC, Seoul Vol.2, pp.577-582 (1989)
- (7) M. Sasaki and H. Inooka, " Application of Inverse Dynamics for Hybrid Translational Position / Force Control of a Flexible Robot Arm," '89 KACC, Seoul vol.2, pp.595-599 (1989)
- (8) K.H.Yu, "An Analysis and Vibration Control of the Translational Motion on the 1-link Flexible Arm," MS.D.Thesis,Aug.1990, Chonbuk National University. (in Korean)
- (9) W.T.Weeks, "Numerical inversion of Laplace Transforms using Laguerre functions," J.of the Association for computing machinery," Vol.13 No.3 pp.419-426.(1966)
- (10) W.J.Book, O.Maizza-Neto and D.E. Whitney, "Feed-back Control of Two Beams, Two Joint Systems with Distributed Flexibility," Trans.of the ASME, 99, pp.424-431.(1975)

APPENDIX

The a_{ij} 's in equation (12) are given as

$$a_{11} = 0$$

$$a_{12} = a_{13} = 1$$

$$a_{21} = J_p s^2 \zeta (\cos \zeta L - \cosh \zeta L) - EI(1+Cs) \zeta^2 (\sin \zeta L + \sinh \zeta L)$$

$$a_{22} = -J_p s^2 \zeta \sin \zeta L - EI(1 + Cs) \zeta^2 \cos \zeta L$$

$$a_{23} = J_p s^2 \zeta \sinh \zeta L + EI(1 + Cs) \zeta^2 \cosh \zeta L$$

$$a_{31} = M_p s^2 (\sin \zeta L - \sinh \zeta L) + EI(1+Cs) \zeta^3 (\cos \zeta L + \cosh \zeta L)$$

$$a_{32} = M_p s^2 \cos \zeta L - EI(1 + Cs) \zeta^3 \sin \zeta L$$

$$a_{33} = M_p s^2 \cosh \zeta L - EI(1 +Cs) \zeta^3 \sinh \zeta L$$